Static Gain, Optical Modulation Response, and Nonlinear Phase Noise in Saturated Quantum-Dot Semiconductor Optical Amplifiers

Xiaoxu Li and Guifang Li, *Senior Member, IEEE*

***Abstract*—A rate equation model preserving charge neutrality for quantum-dot semiconductor optical amplifiers (QD-SOAs) is established to investigate the nonlinear gain dynamics in the saturation regime. The static gain of QD-SOA is calculated assuming overall charge neutrality and compared with that without overall charge neutrality. Optical modulation response and nonlinear phase fluctuation through saturated QD-SOAs are calculated numerically based on a small-signal analysis. The gain dynamics of QD-SOAs are strongly dependent on the current injection level. The carrier reservoir in the wetting layer and continuum state is necessary for QD-SOAs to operate with high gain, high saturation power, and ultrafast gain recovery.**

***Index Terms*—Gain recovery, modulation response, phase noise, quantum dots (QDs), semiconductor optical amplifiers (SOAs).**

I. Introduction

QUANTUM-DOT (QD) devices have attracted great attention in recent years because of their high differential gain and fast relaxation into the active state from the barrier and wetting layer (WL) [1]. QD semiconductor optical amplifiers (SOA) can potentially offer many advantages over bulk and quantum-well (QW) counterparts, resulting primarily from three-dimensional (3-D) quantum confinement of electrons and holes in quantum dots. Ultrafast gain recovery time of the order of 100 fs has been observed in QD-SOAs, which makes them ideal for ultrafast signal processing [2]. Recently, QD-SOAs with high gain, high saturation power, and low noise figure over an ultrawide gain spectrum of 120 nm have been developed as a cost-effective alternative to erbium-doped fiber amplifiers (EDFAs) for optical transmission [3].

As is with the electrical modulation response of QD lasers [4], [5], the optical modulation response of QD-SOAs is important because it is directly related to the gain fluctuation and, through the linewidth-enhancement factor (LEF) or chirp factor α_H [6], the nonlinear phase noise, which in turn determines the performance of transmission systems for phase-modulated signal such as differential-phase-shift-keying (DPSK) using SOAs for optical amplification or regeneration [7]. In this paper, we present a QD-SOA model for carrier relaxation and excitation among QD energy states and WL, taking into account overall charge neutrality for the whole device. The dc characteristics of QD-SOA are studied first followed by an analysis of small-signal ac modulation characteristics. The effective carrier lifetime and saturation output power are derived. Finally, the optical modulation response and nonlinear phase fluctuation in saturated QD-SOAs are calculated.

Manuscript received June 10, 2008; revised October 20, 2008. Current version published April 03, 2009.

The authors are with CREOL, The College of Optics and Photonics, University of Central Florida, Orlando, FL 32816 USA (e-mail: xiali@creol.ucf.edu; li@creol.ucf.edu).

Digital Object Identifier 10.1109/JQE.2009.2013100

II. Theory

A. Rate Equation Model for QD-SOA

The QDs are assumed to have two discrete energy states, i.e., ground state (GS) and excited state (ES), and a continuum state (CS), which is an ensemble of dense excited states in each dot. Different dots are interconnected through a two-dimensional (2-D) WL. Our model ignores barrier dynamics and assumes the electrons are injected directly into the WL, then captured by the CS and finally relaxed into the ES and GS. The corresponding rate equations describing the change in carrier (electron) densities in the WL (N_w), CS (N_c), ES (N_2), and GS (N_1), which are all normalized to the active region volume, can be written as [2], [8]–[11]

$$\frac{\partial N_w}{\partial t} = \frac{J}{eL_w} - \frac{N_w(1-f_c)}{\tau_{wc}} + \frac{N_c(1-f_w)}{\tau_{cw}} - \frac{N_w}{\tau_{wR}} \tag{1}$$

$$\frac{\partial N_c}{\partial t} = \frac{N_w(1-f_c)}{\tau_{wc}} - \frac{N_c(1-f_w)}{\tau_{cw}} + \frac{N_2(1-f_c)}{\tau_{2c}} - \frac{N_c(1-f_2)}{\tau_{c2}} + \frac{N_1(1-f_c)}{\tau_{1c}} - \frac{N_c(1-f_1)}{\tau_{c1}} \tag{2}$$

$$\frac{\partial N_2}{\partial t} = \frac{N_c(1-f_2)}{\tau_{c2}} - \frac{N_2(1-f_c)}{\tau_{2c}} + \frac{N_1(1-f_2)}{\tau_{12}} - \frac{N_2(1-f_1)}{\tau_{21}} \tag{3}$$

$$\frac{\partial N_1}{\partial t} = \frac{N_c(1-f_1)}{\tau_{c1}} - \frac{N_1(1-f_c)}{\tau_{1c}} + \frac{N_2(1-f_1)}{\tau_{21}} - \frac{N_1(1-f_2)}{\tau_{12}} - \frac{N_1 h_1}{\tau_{1R}} - \frac{gP}{\sigma\hbar\omega} \tag{4}$$

where J is the injection current density, e is the electron charge, L_w is the thickness of the WL, $\hbar\omega$ is the photon energy corresponding to the GS transition, P is the optical power, and σ is the cross section of the active region. Electron occupation probabilities f_w, f_c, f_2, and f_1 correspond to the WL, CS, ES, and GS, respectively, and are related to electron densities by

$$\begin{aligned} N_w &= 2D_w\tilde{N}_Q f_w \\ N_c &= 2D_c\tilde{N}_Q f_c \\ N_2 &= 2D_2\tilde{N}_Q f_2 \\ N_1 &= 2D_1\tilde{N}_Q f_1 \end{aligned} \tag{5}$$

where D_w, D_c, D_2, and D_1 are the degeneracies of the corresponding electron states. The factor of two is from electron spin. The effective volume density of the QDs is $\tilde{N}_Q$, given by $\tilde{N}_Q = N_Q/L_w$, where N_Q is the surface density of QDs. The modal gain in GS is g, given by $g = g_{\max}(f_1 + h_1 - 1)$, where $g_{\max}$ is the maximum modal gain, which depends on the confinement factor of each QD, the surface density of QDs, and the number of QD layers. The hole occupation probability in the GS in the valence band of QDs is h_1. The electron spontaneous recombination lifetimes in the WL and the GS are τ_{wR} and τ_{1R}, respectively. The electron capture time from the WL to the CS is τ_{wc} and described by

$$\tau_{wc} = \frac{\tau_{wc0}}{1 + C_{wc} f_w} \tag{6}$$

where τ_{wc0} is the electron capture time solely associated with the phonon-assisted process, C_{wc} is the dimensionless ratio of the Auger-assisted coefficient to the phonon-assisted coefficient in the capture process. The electron escape time from the CS to the WL is τ_{cw} and can be expressed, under the condition of thermal equilibrium, by

$$\tau_{cw} = \tau_{wc} \exp\left(\frac{\Delta E^c_{wc}}{kT}\right) \tag{7}$$

where ΔE^c_{wc} is the energy separation between the WL bandedge and the CS in the conduction band of QDs and kT is the thermal energy at room temperature. The same relationship is applied to the intradot relaxations and excitations thereby the intradot relaxation and excitation times in (2)–(4) can be expressed as

$$\tau_{ij} = \frac{\tau_{ij0}}{1 + C_{ij} f_w}$$
$$\tau_{ji} = \frac{D_j}{D_i} \exp\left(\frac{\Delta E^c_{ij}}{kT}\right) \tau_{ij}, \qquad i = c, 2;\ j = 2, 1;\ i \neq j \tag{8}$$

where τ_{ij0} is the phonon-dominated relaxation time and C_{ij} is the dimensionless ratio of the Auger-assisted coefficient to the phonon-assisted coefficient in the relaxation processes, and ΔE^c_{ij} is the energy separation between the ith state and the jth state in the conduction band of QDs. Assuming "k-conservation" in the interband transition, ΔE^c_{ij} can be written by

$$\Delta E^c_{ij} = \frac{m^*_h}{m^*_e} \Delta E^v_{ij}, \qquad i, j = w, c, 2, 1 \text{ and } i \neq j \tag{9}$$

where ΔE^v_{ij} is the energy separation between the corresponding hole states in the valence band of QDs and m^*_e and m^*_h are the effective masses of electron and hole, respectively.

B. Overall Charge Neutrality of QD-SOA

The overall charge neutrality of QD-SOA can be described by

$$D_1 f_1 + D_2 f_2 + D_c f_c + D_w f_w = D_1 h_1 + D_2 h_2 + D_c h_c + D_w h_w \tag{10}$$

where h_w, h_c, and h_2 are the hole occupation probabilities in the WL bandedge, CS, and ES in the valance band of QDs, respectively. Due to the larger effective mass of holes and the resulting small separation between energy levels, holes can be assumed to be in equilibrium all times over the entire valence band. The hole occupation probabilities satisfy the Fermi–Dirac distribution and can be written as

$$h_i = \frac{1}{1 + \exp\left[-\left(\frac{E^v_i - E^v_f}{kT}\right)\right]}, \qquad i = w, c, 2, 1 \tag{11}$$

where E^v_i is the hole energy level and E^v_f is the quasi-Fermi level of the valence band. The hole occupation probabilities at upper levels can be further expressed as that in the ground state

$$h_i = \frac{1}{1 + \exp\left(\frac{\Delta E^v_{i1}}{kT}\right)\left(h_1^{-1} - 1\right)}, \qquad i = w, c, 2 \tag{12}$$

where ΔE^v_{i1} is the energy separation between the band edge of the WL, CS, or ES, and the GS in the valence band. It is also assumed in (10) that the electron states in the conduction band and corresponding hole states in the valence band have identical degeneracies assuming "k-conservation" in the transition.

C. Steady-State Solution

For a CW incident on the QD-SOA, (1)–(4) can be solved by setting the left-hand side to zero. At a given optical power $\overline{P}$ and employing (10) and (12), the electron occupation probability ($\overline{f}_1$) and hole occupation probability ($\overline{h}_1$) in the GS can be solved. Knowing $\overline{f}_1$ and $\overline{h}_1$, the upper level electron occupation probabilities and modal gain can be written as

$$\overline{f}_w = \frac{\tau_{wR}}{D_w \tau_{1R}}\left[I_0 - D_1 \overline{f}_1 \overline{h}_1 - \frac{1}{2}(\overline{f}_1 + \overline{h}_1 - 1)\frac{\overline{P}}{P_{\text{sat0}}}\right] \tag{13}$$

$$\overline{f}_c = \frac{D_w \overline{f}_w \left(\frac{1}{\tau_{wR}} + \frac{1}{\tau_{wc}}\right) - \frac{I_0}{\tau_{1R}}}{\frac{D_w \overline{f}_w}{\tau_{wc}} + \frac{D_c(1 - \overline{f}_w)}{\tau_{cw}}} \tag{14}$$

$$\overline{f}_2 = \frac{\frac{D_c \overline{f}_c}{\tau_{c2}} + \frac{D_1 \overline{f}_1}{\tau_{12}}}{\frac{D_c \overline{f}_c}{\tau_{c2}} + \frac{D_1 \overline{f}_1}{\tau_{12}} + \frac{D_2(1 - \overline{f}_c)}{\tau_{2c}} + \frac{D_2(1 - \overline{f}_1)}{\tau_{21}}} \tag{15}$$

$$\overline{g} = g_{\max}(\overline{f}_1 + \overline{h}_1 - 1) \tag{16}$$

where I_0 is the normalized injection current to the amplifier, given by

$$I_0 = \frac{\tau_{1R}}{2eN_Q} J. \tag{17}$$

P_{sat0} is an intrinsic parameter related to the saturation output power of the amplifier and can be expressed as

$$P_{\text{sat0}} = \frac{\hbar\omega}{\tau_{1R}} \frac{\sigma \tilde{N}_Q}{g_{\max}}. \tag{18}$$

In a traveling-wave QD-SOA, the evolution of optical power ($\overline{P}$) can be described by [12]

$$\frac{\partial \overline{P}}{\partial z} - \frac{1}{v_g}\frac{\partial \overline{P}}{\partial t} = (g - \alpha_{\text{int}})\overline{P} \tag{19}$$

where v_g is the group velocity and α_{int} is the internal loss coefficient. Based on the above equation and the steady-state solutions, the optical power and carrier densities along the longitudinal SOA can be calculated numerically through iterations.

D. Small-Signal Analysis

The small-signal dynamics of QD-SOA are now investigated through a perturbation analysis. To do so, the power, carrier occupation probabilities, and modal gain are assumed to be of the form

$$\begin{aligned} P &= \overline{P} + \Delta P \\ f_w &= \overline{f}_w + \Delta f_w \\ f_c &= \overline{f}_c + \Delta f_c \\ f_2 &= \overline{f}_2 + \Delta f_2 \\ f_1 &= \overline{f}_1 + \Delta f_1 \\ h_1 &= \overline{h}_1 + \Delta h_1 \\ g &= \overline{g} + \Delta g \end{aligned} \tag{20}$$

where $\overline{P}$, $\overline{f}_w$, $\overline{f}_c$, $\overline{f}_2$, $\overline{f}_1$, $\overline{h}_1$, and $\overline{g}$ are steady-state solutions to (1)–(4) and (10). Substituting (20) into (1)–(4) and (10) and neglecting higher order terms, the perturbation terms satisfy the following linear differential equations:

$$\frac{d}{dt}\begin{pmatrix} \Delta f_w \\ \Delta f_c \\ \Delta f_2 \\ \Delta f_1 \end{pmatrix} = \begin{pmatrix} c_{ww} & c_{wc} & c_{w2} & c_{w1} \\ c_{cw} & c_{cc} & c_{c2} & c_{c1} \\ c_{2w} & c_{2c} & c_{22} & c_{21} \\ c_{1w} & c_{1c} & c_{12} & c_{11} \end{pmatrix} \begin{pmatrix} \Delta f_w \\ \Delta f_c \\ \Delta f_2 \\ \Delta f_1 \end{pmatrix} + \begin{pmatrix} 0 \\ 0 \\ 0 \\ -\frac{\overline{g}}{2g_{\max}\tau_{1R}}\frac{\Delta P}{P_{\text{sat0}}} \end{pmatrix} \tag{21}$$

where each element of the 4×4 matrix (C) is a function of the steady-state solutions. The solutions to (21) have the form

$$\begin{aligned} \begin{pmatrix} \Delta f_w \\ \Delta f_c \\ \Delta f_2 \\ \Delta f_1 \end{pmatrix} =& A_w \begin{pmatrix} z_{ww} \\ z_{cw} \\ z_{2w} \\ z_{1w} \end{pmatrix} e^{\lambda_w t} + A_c \begin{pmatrix} z_{wc} \\ z_{cc} \\ z_{2c} \\ z_{1c} \end{pmatrix} e^{\lambda_c t} \\ &+ A_2 \begin{pmatrix} z_{w2} \\ z_{c2} \\ z_{22} \\ z_{12} \end{pmatrix} e^{\lambda_2 t} + A_1 \begin{pmatrix} z_{w1} \\ z_{c1} \\ z_{21} \\ z_{11} \end{pmatrix} e^{\lambda_1 t} + \begin{pmatrix} p_w(t) \\ p_c(t) \\ p_2(t) \\ p_1(t) \end{pmatrix}. \end{aligned} \tag{22}$$

The first four terms on the right-hand side of (22) denote the general solution and the transient process, in which λ_w, λ_c, λ_2, and λ_1 are the eigenvalues of C corresponding to normalized eigenvectors of $Z_i = (z_{wi}, z_{ci}, z_{2i}, z_{1i})^T$, $i = w, c, 2, 1$; A_w, A_c, A_2, and A_1 are the coefficients determined by the initial conditions. The last term in (22) represents the particular solution to (21) and describes fluctuations of the carrier densities and modal gain after a long observing time. It can be expressed as

$$\begin{pmatrix} p_w(t) \\ p_c(t) \\ p_2(t) \\ p_1(t) \end{pmatrix} = \begin{pmatrix} z_{ww}e^{\lambda_w t} & z_{wc}e^{\lambda_c t} & z_{w2}e^{\lambda_2 t} & z_{w1}e^{\lambda_1 t} \\ z_{cw}e^{\lambda_w t} & z_{cc}e^{\lambda_c t} & z_{c2}e^{\lambda_2 t} & z_{c1}e^{\lambda_1 t} \\ z_{2w}e^{\lambda_w t} & z_{2c}e^{\lambda_c t} & z_{22}e^{\lambda_2 t} & z_{21}e^{\lambda_1 t} \\ z_{1w}e^{\lambda_w t} & z_{1c}e^{\lambda_c t} & z_{12}e^{\lambda_2 t} & z_{11}e^{\lambda_1 t} \end{pmatrix} \times \begin{pmatrix} s_w(t) \\ s_c(t) \\ s_2(t) \\ s_1(t) \end{pmatrix} \tag{23}$$

where $S(t) = (s_w(t)\ s_c(t)\ s_2(t)\ s_1(t))^T$ satisfies

$$\frac{d}{dt}\begin{pmatrix} s_w(t) \\ s_c(t) \\ s_2(t) \\ s_1(t) \end{pmatrix} = \begin{pmatrix} v_{ww}e^{-\lambda_w t} & v_{wc}e^{-\lambda_w t} & v_{w2}e^{-\lambda_w t} & v_{w1}e^{-\lambda_w t} \\ v_{cw}e^{-\lambda_c t} & v_{cc}e^{-\lambda_c t} & v_{c2}e^{-\lambda_c t} & v_{c1}e^{-\lambda_c t} \\ v_{2w}e^{-\lambda_2 t} & v_{2c}e^{-\lambda_2 t} & v_{22}e^{-\lambda_2 t} & v_{21}e^{-\lambda_2 t} \\ v_{1w}e^{-\lambda_1 t} & v_{1c}e^{-\lambda_1 t} & v_{12}e^{-\lambda_1 t} & v_{11}e^{-\lambda_1 t} \end{pmatrix} \times \begin{pmatrix} 0 \\ 0 \\ 0 \\ -\frac{\overline{g}}{2g_{\max}\tau_{1R}}\frac{\Delta P}{P_{\text{sat0}}} \end{pmatrix} \tag{24}$$

where $V = (Z_w, Z_c, Z_2, Z_1)^{-1}$. The above equation can be solved analytically in the frequency domain assuming $\Delta P(z,t) = \Delta P(z)e^{j\omega t}$. Ignoring the transient process, the relative gain fluctuation is associated with the relative power fluctuation at an arbitrary position of a QD-SOA through

$$\frac{\Delta g(z,\omega)}{\overline{g}(z)} = F(z,\omega)\frac{\Delta P(z)}{\overline{P}(z)}. \tag{25}$$

Here, $F(z,\omega)$ exactly shows the optical modulation response of the QD-SOA and can be expressed by

$$F(z,\omega) = -\left(\frac{X_w\tau_w}{1+j\omega\tau_w} + \frac{X_c\tau_c}{1+j\omega\tau_c} + \frac{X_2\tau_2}{1+j\omega\tau_2} + \frac{X_1\tau_1}{1+j\omega\tau_1}\right)\cdot\frac{1}{2\tau_{1R}}\frac{\overline{P}(z)}{P_{\text{sat0}}} \tag{26}$$

where

$$X_i = \left[\alpha_w z_{wi} + \alpha_c z_{ci} + \alpha_2 z_{2i} + (1+\alpha_1)z_{1i}\right]v_{i1}, \quad i = w, c, 2, 1 \tag{27}$$

$$\alpha_j = \frac{D_j}{D_w H_w + D_c H_c + D_2 H_2 + D_1 H_1}, \quad j = w, c, 2, 1 \tag{28}$$

$$H_w = \frac{\exp\left(\Delta E^v_{w1}/kT\right)}{\left[\overline{h}_1 + \exp\left(\Delta E^v_{w1}/kT\right)(1-\overline{h}_1)\right]^2} \tag{29}$$

$$H_c = \frac{\exp\left(\Delta E^v_{c1}/kT\right)}{\left[\overline{h}_1 + \exp\left(\Delta E^v_{c1}/kT\right)(1-\overline{h}_1)\right]^2} \tag{30}$$

$$H_2 = \frac{\exp\left(\Delta E^v_{21}/kT\right)}{\left[\overline{h}_1 + \exp\left(\Delta E^v_{21}/kT\right)(1-\overline{h}_1)\right]^2} \tag{31}$$

$$H_1 = 1 \tag{32}$$

The minus sign on the right-hand side of (26) indeed reflects the gain saturation of QD-SOA, i.e., the increasing power will lead to the decreasing gain. It is clearly seen that the optical modulation response of the QD-SOA is composed of four low-pass frequency responses, which have characteristic times of τ_w, τ_c, τ_2, and τ_1, corresponding to the contributions from WL, CS, ES, and GS, respectively, where $\tau_i = -\lambda_i^{-1}$, $i = w, c, 2, 1$. The contribution of each term to the total modulation response is weighed by the corresponding coefficient ($X_i, i = w, c, 2, 1$ and $\sum_i X_i \approx 1$). Now, applying the small-signal analysis to (19), one can write the propagation equation of the power fluctuation as

$$\frac{\partial \Delta P}{\partial z} - \frac{j\omega}{v_g}\Delta P = (\overline{g} - \alpha_{\text{int}})\Delta P + \overline{P}\Delta g. \tag{33}$$

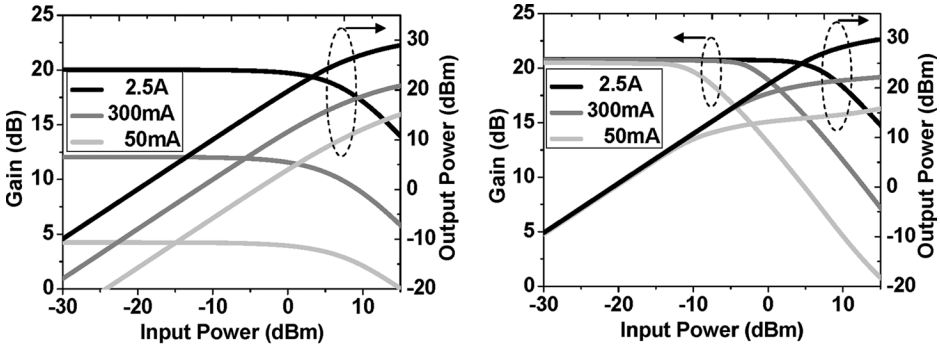

Fig. 1. Optical gain and output power of QD-SOA as functions of input power with (a) charge neutrality for whole device and (b) charge neutrality in GS only.

Solving (25) and (33) analytically, the position-dependent gain fluctuation is given by

$$\frac{\Delta g(z,\omega)}{\overline{g}(z)} = F(z,\omega)\exp\left\{\int_0^z F(z',\omega)\overline{g}(z')dz'\right\}e^{j\omega\frac{z}{v_g}}\frac{\Delta P(0)}{\overline{P}(0)} \tag{34}$$

where $\Delta P(0)/\overline{P}(0)$ is the relative power fluctuation at the input of QD-SOA and $\overline{g}(z)$ is the position-dependent modal gain in steady-state.

E. Nonlinear Phase Fluctuation (Noise) Through Saturated QD-SOA

It is known that carrier density or gain in SOA introduces a nonlinear phase shift $\phi(\tau)$ to the light wave, which is directly related to the gain $g(z,\tau)$ through [13]

$$\phi(\tau) = -\frac{1}{2}\alpha_H\int_0^L g(z,\tau)dz \tag{35}$$

where α_H is the LEF or chirp factor at GS transition wavelength, $g(z,\tau)$ is the time- and position-dependent modal gain and $\tau = t - z/v_g$. In the saturation regime of QD-SOA, if the input optical power varies with time, e.g., from signal-ASE beat noise, $g(z,\tau)$ and $\phi(\tau)$ will also contain a time-varying component. The nonlinear phase fluctuation or noise through saturated QD-SOA can be described by

$$\Delta\phi_{NL}(\tau) = -\frac{1}{2}\alpha_H\int_0^L \Delta g(z,\tau)dz \tag{36}$$

and the frequency-dependent nonlinear phase fluctuation can be further written as

$$\Delta\phi_{NL}(\omega) = -\frac{1}{2}\alpha_H\int_0^L \Delta g(z,\omega)e^{-j\omega\frac{z}{v_g}}dz. \tag{37}$$

III. Results and Discussions

In order to study the gain dynamics and optical modulation response of QD-SOAs, (1)–(4), (10), and (19) are solved numerically. The parameters used in simulation are [2], [5], [8]–[10], [14]: $L = 3$ mm (length of the waveguide), $L_w = 200$ nm, $W = 10$ μm (strip width of the waveguide); $N_Q = 5\times10^{10}$ cm^{-2}, $g_{\max} = 19$ cm^{-1}, $\alpha_{\text{in}} = 3$ cm^{-1}; $D_1 = 1$, $D_2 = 3$, $D_c = 10$, $D_w = 250$; $\tau_{wc0} = 1$ ps, $\tau_{c20} = \tau_{c10} = \tau_{210} = 10$ ps, $\tau_{1R} = 1$ ns; $C_{wc} = 0.25$, $C_{c2} = C_{21} = 50$, $C_{c1} = 15$; $m_e^* = 0.026\,m_0$, and $m_h^* = 0.0742\,m_0$, where m_0 is the electron mass. As in [2] and [14], we take the interband transition energies of the excited state, continuum state and band edge of the WL as $\hbar\omega + 70$ meV, $\hbar\omega + 150$ meV and $\hbar\omega + 180$ meV, respectively, where $\hbar\omega$ is the photon energy corresponding to the ground-state transition.

Fig. 1(a) shows the dependence of the gain and the output power of QD-SOA on the input power at different injection currents when charge neutrality for whole device is assumed. Taking into account the Auger recombination, the electrons spontaneous recombination lifetimes in the WL (τ_{wR}) are 1, 0.8, and 0.4 ns, respectively, at injection currents of 50 mA, 300 mA, and 2.5 A. It is clearly shown that the small-signal gain or the unsaturated gain increases significantly from 4.2 dB at 50 mA to 20 dB at 2.5 A. It is noted that the SOA gain is proportional to the population inversion in GS, i.e., $f_1 + h_1 - 1$. The small unsaturated gain at low injection current is attributed to low hole occupation in GS (h_1) resulting in low population inversion because of the thermal equilibrium among the closely spaced hole states. The similar condition has already been studied for QD lasers, which usually operate at low injection current, and it is proved that the population inversion and gain of QD lasers can be enhanced by p-doping the dots [15]. For comparison, Fig. 1(b) shows the dependence of the gain and the output power of QD-SOA on the input power at the same injection current levels while charge neutrality is only assumed in GS, i.e., $f_1 = h_1$. It is clearly seen in Fig. 1(b) that this simple assumption overestimates the unsaturated gain at low injection level [16] and only becomes valid for QD-SOAs with high injection current. Hence, the overall charge neutrality of QD-SOA is adopted in the following studies of gain dynamics. In Fig. 1(a), the optical gain starts to saturate as the optical power increases because of the carrier depletion in the QDs. The saturation output power increases as the injection current increases due to the increase of the carrier densities in the WL as well as QDs. However, it is eventually limited by the density of dots and the finite carrier capture and relaxation times. The injection currents of $I = 50$ mA and $I = 2.5$ A corresponding to current densities of 0.17 kA $\cdot$ cm^{-2} and 8.3 kA $\cdot$ cm^{-2},

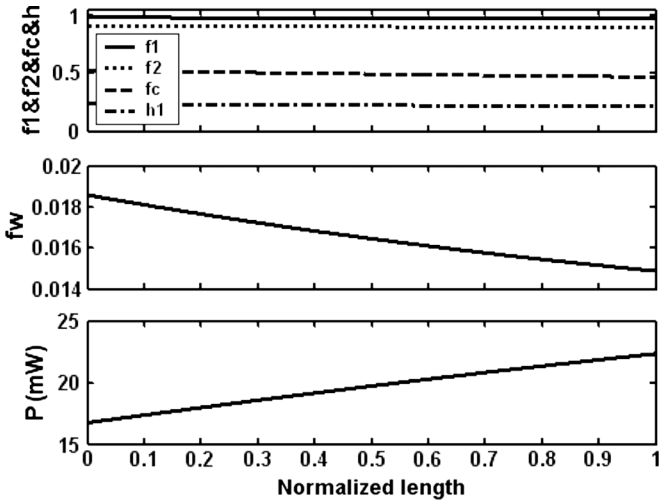

Fig. 2. Electron occupation probability in GS (f_1), ES (f_2), CS (f_c) and hole occupation probability in GS (h_1) (top); electron occupation probability in WL (f_w) (middle) and optical power (bottom) as a function of the normalized QD-SOA length at $I = 50$ mA and $\overline{P}(0) = 12.2$ dBm.

respectively, are adopted in the following simulations to represent low and high injection level into the QD-SOA. The corresponding saturation output powers are 13.5 dBm and 27.2 dBm, respectively.

A. Low Injection Level

Fig. 2 shows the evolution of the optical power of a CW signal and the carrier densities in QDs and WL along the normalized SOA length at the injection current of 50 mA. The optical input power is 12.2 dBm leading to a gain of 1.2 dB, which is 3 dB lower than the unsaturated gain. It is seen in Fig. 2 that hole occupation probability in GS (h_1) is small due to the low injection current, which leads to a weak population inversion of carriers in GS and small modal gain of SOA. The carriers in QDs are depleted gradually and signal power increases linearly when the signal propagates along the SOA.

The optical modulation response described by (26) is plotted as a function of modulation frequency in Fig. 3. The total modulation response (solid line) is composed of four low-pass frequency responses, which are the contributions to the dynamics due to WL, CS, ES, and GS, respectively. At the input of the QD-SOA, shown in Fig. 3(a), the calculated characteristic times corresponding to the contributions from WL, CS, ES and GS are 7.7 fs, 47.6 ps, 0.80 ps, and 0.64 ps, respectively. It is clearly shown that the total modulation response of the QD-SOA is dominated by the low-pass frequency response of the continuum state and the effective characteristic time or gain recovery time of the QD-SOA is 47.6 ps. Similarly, the optical modulation at the output of the QD-SOA, shown in Fig. 3(b), is also dominated by the CS low-pass frequency response and the gain recovery time of QD-SOA is 50.4 ps. The slow modulation response or gain recovery is attributed to the insufficient carriers supplied into the QDs because of the small injection current. Therefore, the gain dynamics of the QD-SOA is dominated by the carrier density pulsation (CDP), which also limits the modulation speed of the bulk and QW SOAs [17]. Similar gain dynamics

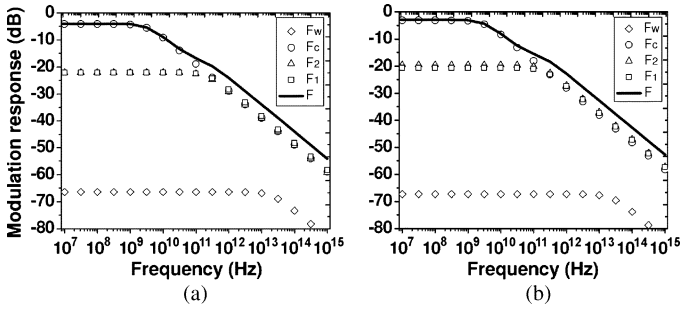

Fig. 3. Optical modulation response of QD-SOA at $I = 50$ mA and (a) $\overline{P}(0) = 12.2$ dBm and (b) $\overline{P}(L) = 13.4$ dBm. The contributions to the total modulation response (solid line) due to WL, CS, ES, and GS are represented by diamond, circle, triangle and square, respectively.

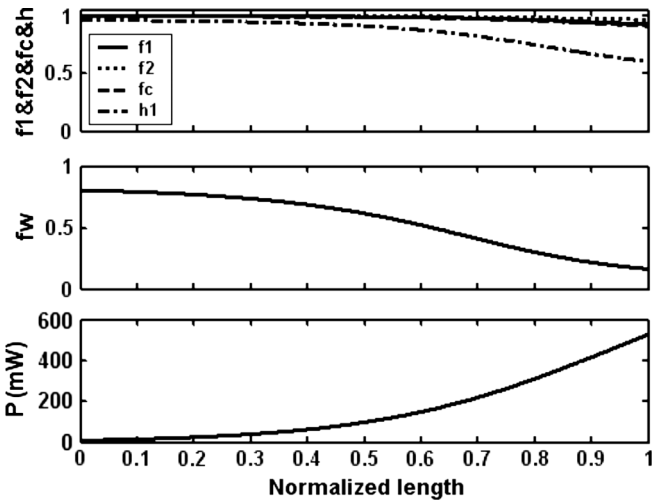

Fig. 4. Electron occupation probability in GS (f_1), ES (f_2), CS (f_c) and hole occupation probability in GS (h_1) (top); electron occupation probability in WL (f_w) (middle) and optical power (bottom) as a function of the normalized QD-SOA length at $I = 2.5$ A and $\overline{P}(0) = 10.2$ dBm.

of QD-SOAs under low injection current as bulk- or QW-SOAs such as data pattern effect has been shown in [9].

B. High Injection Level

In Fig. 4, the evolution of the carrier densities and the optical power are studied again at higher injection current of 2.5 A. The input power of 10.2 dBm is incident onto QD-SOA to have a gain of 17 dB with the same gain suppression as that in Fig. 2. Both electrons and holes in QDs are fully populated at the input of the SOA because of the weak stimulated emission and high injection current. Thus, the signal experiences high gain and signal power increases exponentially. As the power increases, the electrons in GS are depleted first because of stimulated emission then the electrons in higher energy states and WL are depleted subsequently due to the refilling into the lower energy states. Meanwhile, the holes in GS of the dots experience faster depletion than the electrons, which further weakens population inversion in GS and the QD-SOA enters the saturation regime eventually.

Fig. 5 shows the optical modulation response at the input and output of the QD-SOA when the driving current is 2.5 A and the average input power is 10.2 dBm. The optical modulation response in Fig. 5(b) is stronger than that in Fig. 5(a) because

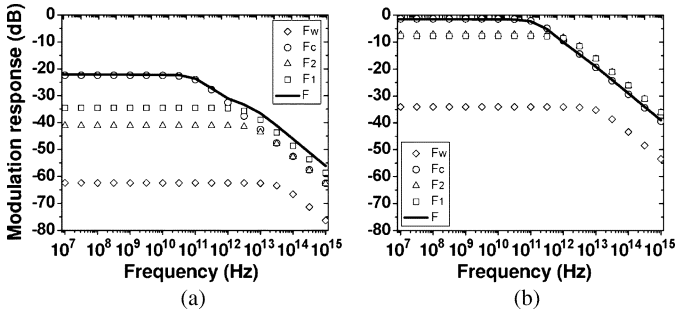

Fig. 5. Optical modulation response of QD-SOA at $I = 2.5$ A and (a) $\overline{P}(0) = 10.2$ dBm and (b) $\overline{P}(L) = 27.2$ dBm. The contributions to the total modulation response (solid line) due to WL, CS, ES, and GS are represented by diamond, circle, triangle, and square, respectively.

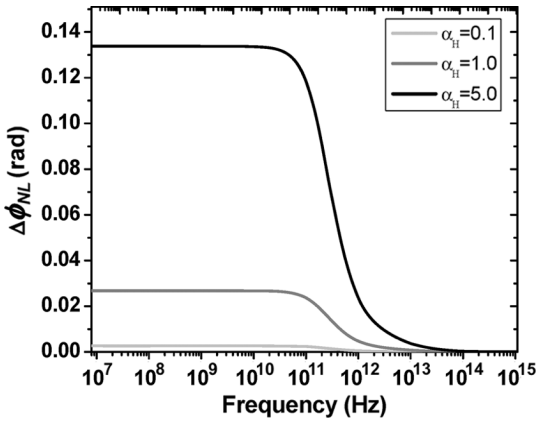

Fig. 6. Frequency response of the accumulated nonlinear phase fluctuation through the saturated QD-SOA. $I = 2.5$ A, $\overline{P}(0) = 10.2$ dBm, and $\Delta\overline{P}(0)/\overline{P}(0) = 0.1$.

of the higher optical power and stronger gain saturation at the output. It is observed from Fig. 3 and Fig. 5 that the optical modulation response of QD-SOA, defined as the relative gain fluctuation to the relative power fluctuation, is always governed by the frequency response of CS, which is characterized by τ_c in (26). Hence, (26) can be approximated by

$$F(z,\omega) \approx -\frac{X_c\tau_c}{1+j\omega\tau_c}\frac{1}{2\tau_{1R}}\frac{\overline{P}(z)}{P_{\text{sat0}}}. \tag{38}$$

Analogous to bulk- and QW-SOAs, the effective gain recovery time and saturation output power of QD-SOA can be written as

$$\tau_{\text{eff,c}} \approx \tau_c \quad P_{\text{sat}} \approx \frac{\hbar\omega}{X_c\tau_c}\frac{\sigma\tilde{N}_Q}{g_{\max}}. \tag{39}$$

The calculated effective gain recovery time is 1.6 ps at the input of the QD-SOA [Fig. 5(a)], which is dominated by the intradot relaxation. The calculated gain recovery time at the output of the QD-SOA in Fig. 5(b) is 1.0 ps. This faster gain recovery at the output of the QD-SOA is due to stronger stimulated emission. Faster gain recovery of ~0.1 ps can be achieved at higher optical power, which is consistent with the experimental measurement in [18].

Based on (34) and (37), the dependence of the total nonlinear phase fluctuation introduced by the saturated QD-SOA on the small-signal modulation frequency is calculated and plotted in Fig. 6 for different LEFs. Apparently, the frequency response of nonlinear phase fluctuation through QD-SOA shows similar low-pass features as the optical modulation response of QD-SOA, described by (26). The nonlinear phase fluctuation is proportional to the LEF of QD-SOA, which can be from as small as 0.1 to more than 10, depending on the injection current, temperature, photon energy, to name a few [19]–[21]. At the LEF of 5.0, shown in Fig. 6, the amplitude of the accumulated nonlinear phase fluctuation is up to 0.133 rad (0.266 rad or 15.2 degrees in terms of peak-to-peak) for small modulation slower than 40 GHz, which is detrimental to the phase-modulated signals in optical communications operating at 10 or 40 Gbit/s and using QD-SOAs for optical amplifications.

IV. Conclusion

The gain dynamics and optical modulation response in saturated QD-SOAs taking into account the overall charge neutrality have been studied both analytically and numerically. Based on the steady-state solution to and small-signal analysis of the rate equation model, the optical modulation response of QD-SOAs is analyzed semi-analytically, which features a low-pass filtering. Similarly as in bulk- and QW-SOAs, the gain recovery time and saturation output power of QD-SOAs are derived. Compared to the conventional SOAs, QD-SOAs have more complicated gain dynamics due to stronger couplings among the WL, CS, ES, and GS. The characteristic times are not only dependent on the transition time and carrier lifetime, but also dependent on the carrier densities in WL and CS. Hence, the current injection level plays an important role in gain saturation and dynamics of QD-SOAs. When the injection current (density) is low, the WL is not fully occupied thus is not able to refill the lower states promptly after the carriers in lower states are depleted by the strong stimulated emission. The gain recovery time is eventually limited by the carrier lifetime and CDP is dominant. In this case, QD-SOAs show similar performance as bulk- or QW-SOAs, i.e., small saturation power and slow gain recovery [8]. However, at high injection current (density), the WL remains full as carrier reservoir to the lower states and the population in GS is fully inverted because of the higher quasi-Fermi level. The gain recovery is mainly determined by the downward intradot relaxation. In this case, the QD-SOAs outperform conventional SOAs with higher saturation power and ultrafast gain recovery. Regarding the application of QD-SOAs in optical transmission systems operating at 10 or 40 Gbit/s, the intensity-modulated signals such as on-off keying can be amplified or regenerated without pattern effect due to the ultrafast gain recovery when the QD-SOAs are highly injected. However, for phase-modulated signals such as DPSK, QD-SOAs will introduce the nonlinear phase fluctuations or noise through the SOA chirp and gain saturation.

Acknowledgment

The authors would thank Dr. X. Xie for numerous and helpful discussions.

REFERENCES

[1] M. Sugawara, T. Akiyama, N. Hatori, M. Ishida, H. Ebe, T. Yamamoto, Y. Nakata, and Y. Arakawa, "Recent progress of self-assembled quantum-dot optical devices for optical telecommunication: Temperature-insensitive 10 Gb/s directly modulated lasers and 40 Gb/s signal-regenrative amplifiers," in *Proc. Opt. Fiber Commun. Conf.*, Mar. 5–10, 2006.

[2] M. Sugawara, T. Akiyama, N. Hatori, Y. Nakata, H. Ebe, and H. Ishikawa, "Quantum-dot semiconductor optical amplifiers for high-bit-rate signal processing up to 160 Gb s^{-1} and a new scheme of 3R regenerators," *Meas. Sci. Technol.*, vol. 13, pp. 1683–1691, 2002.

[3] T. Akiyama, M. Ekawa, M. Sugawara, H. Sudo, K. Kawaguchi, A. Kuramata, H. Ebe, K. Morito, H. Imai, and Y. Arakawa, "An ultrawideband (120 nm) semiconductor optical amplifier having an extremely high penalty-free output power of 23 dBm realized with quantum-dot active layers," in *Proc. Opt. Fiber Commun. Conf.*, Feb. 23–27, 2004, vol. 2.

[4] D. Klotzkin and P. Bhattacharya, "Temperature dependence of dynamic and DC characteristics of quantum-well and quantum-dot lasers: A comparative study," *J. Lightw. Technol.*, vol. 17, no. 9, pp. 1634–1642, Sep. 1999.

[5] D. G. Deppe and D. L. Huffaker, "Quantum dimensionality, entropy, and the modulation response of quantum dot lasers," *Appl. Phys. Lett.*, vol. 77, pp. 3325–3327, 2000.

[6] C. H. Henry, "Theory of the linewidth of semiconductor lasers," *IEEE J. Quantum Electron.*, vol. QE-18, no. 2, pp. 259–264, Feb. 1982.

[7] G. Onishchukov, V. Lokhnygin, A. Shipulin, and M. Gölles, "Differential binary phase-shift keying transmission using cascaded semiconductor optical amplifiers," in *Proc. CLEO/Pacific Rim Conf.*, 1999, vol. 2, pp. 513–514.

[8] T. W. Berg, S. Bischoff, I. Magnusdottir, and J. Mørk, "Ultrafast gain recovery and modulation limitations in self-assembled quantum-dot devices," *IEEE Photon. Technol. Lett*, vol. 13, no. 6, pp. 541–543, Jun. 2001.

[9] X. Li and G. Li, "Comments on "Theoretical analysis of gain recovery time and chirp in QD-SOA"," *IEEE Photon. Technol. Lett.*, vol. 18, no. 22, pp. 2434–2435, Nov. 2006.

[10] T. W. Berg and J. Mørk, "Saturation and noise properties of quantum-dot optical amplifiers," *IEEE J. Quantum Electron.*, vol. 40, no. 11, pp. 1527–1539, Nov. 2004.

[11] J. Xiao and Y. Huang, "Numerical analysis of gain saturation, noise figure, and carrier distribution for quantum-dot semiconductor-optical amplifiers," *IEEE J. Quantum Electron.*, vol. 44, no. 5, pp. 448–455, May 2008.

[12] G. P. Agrawal and N. A. Olsson, "Self-phase modulation and spectral broadening of optical pulses in semiconductor laser amplifiers," *IEEE J. Quantum Electron.*, vol. 25, no. 11, pp. 2297–2306, Nov. 1989.

[13] X. Wei and L. Zhang, "Analysis of the phase noise in saturated SOAs for DPSK applications," *IEEE J. Quantum Electron.*, vol. 41, no. 4, pp. 554–561, Apr. 2005.

[14] M. Sugawara, N. Hatori, T. Akiyama, Y. Nakata, and H. Ishikawa, "Quantum-dot semiconductor optical amplifiers for high bit-rate signal processing over 40 Gbit/s," *Jpn. J. Appl. Phys.*, vol. 40, pp. L488–L491, 2001.

[15] D. G. Deppe, H. Huang, and O. B. Schekin, "Modulation characteristics of quantum-dot lasers: The influence of p-typed doping and the electronic density of states on obtaining high speed," *IEEE J. Quantum Electron.*, vol. 38, no. 12, pp. 1587–1593, Dec. 2002.

[16] Z. Bakonyi, H. Su, G. Onishchukov, L. F. Lester, A. L. Gray, T. C. Newell, and A. Tünnermann, "High-gain quantum-dot semiconductor optical amplifier for 1300 nm," *IEEE J. Quantum Electron.*, vol. 39, no. 11, pp. 1409–1414, Nov. 2003.

[17] J. Mørk, A. Mecozzi, and G. Eisenstein, "The modulation response of a semiconductor laser amplifier," *IEEE J. Sel. Topics Quantum Electron.*, vol. 5, no. 3, pp. 851–860, May–Jun. 1999.

[18] P. Borri, W. Langbein, J. M. Hvam, F. Heinrichscorff, M.-H. Mao, and D. Bimberg, "Spectral hole-burning and carrier-heating dynamics in InGaAs quantum-dot amplifiers," *IEEE J. Sel. Topics Quantum Electron.*, vol. 6, no. 3, pp. 544–551, May–Jun. 2000.

[19] T. C. Newell, D. J. Bossert, A. Stinz, A. Fuchs, and K. J. Malloy, "Gain and linewidth enhancement factor in InAs quantum-dot laser diodes," *IEEE Photon. Technol. Lett.*, vol. 11, no. 12, pp. 1527–1529, Dec. 1999.

[20] S. Schneider, P. Borri, W. Langbein, U. Woggon, R. L. Sellin, D. Ouyang, and D. Bimberg, "Linewidth enhancement factor in InGaAs quantum-dot amplifiers," *IEEE J. Quantum Electron.*, vol. 40, no. 10, pp. 1423–1429, Oct. 2004.

[21] J. M. Vázquez, H. H. Nilsson, J.-Z. Zhang, and I. Galbraith, "Linewidth enhancement factor of quantum-dot optical amplifiers," *IEEE J. Quantum Electron.*, vol. 42, no. 10, pp. 986–993, Oct. 2006.

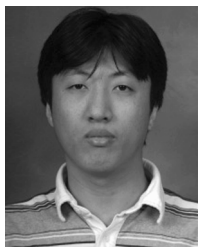

Xiaoxu Li was born in Henan Province, China, in 1977. He received the B.S. and M.E. degrees in electronics from Peking University, Beijing, China, in 1999 and 2002, respectively. He is currently working toward the Ph.D. degree at CREOL, The College of Optics and Photonics, University of Central Florida, Orlando.

His research interests include semiconductor optical amplifiers, wavelength-divisions multiplexing transmission systems, and coherent optical communication.

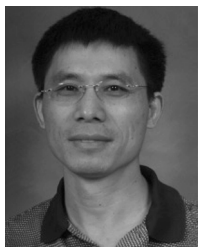

Guifang Li (M'94–SM'06) received the Ph.D. degree in electrical engineering from the University of Wisconsin, Madison, in 1991.

He is a Professor of optics, electrical and computer engineering and physics with the University of Central Florida (UCF), Orlando. His research interests include optical communications and networking, RF photonics and optical processing of time-domain signals. He is the director of the NSF IGERT program in Optical Communications and Networking at UCF.

Dr. Li is a Fellow of the Optical Society of America and SPIE. He was a recipient of the National Science Foundation Career Award and the Office of Naval Research Young Investigator Award.